JACS
JOURNAL OF THE AMERICAN CHEMICAL SOCIETY
Article
pubs.acs.org/JACS

Enhancing Molecular Recognition in Electron Donor–Acceptor Hybrids via Cooperativity

Rafael M. Krick Calderon,[§,‡] Julián Valero,[†,∥,‡] Bruno Grimm,[§] Javier de Mendoza,[†] and Dirk M. Guldi*[,§]

[†]Institute of Chemical Research of Catalonia, Avgda. Països Catalans 16, 43007 Tarragona, Spain
[§]Department of Chemistry and Pharmacy and Interdisciplinary Center for Molecular Materials (ICMM), Friedrich-Alexander-Universität Erlangen-Nürnberg, Egerlandstraße 3, 91058 Erlangen, Germany

Supporting Information

ABSTRACT: Herein, we report the synthesis of guanidinium bis-porphyrin tweezers **1** and fullerene carboxylate **3**, their assembly into a novel supramolecular **1@3** electron donor–acceptor hybrid, and its characterization. In solution, the binding constant affording **1@3** is exceptionally high. **1@3**, which features a highly confined topography, builds up from a combination of guanidinium-carboxylate hydrogen bonding and $\pi-\pi$ stacking/charge-transfer motifs. The latter is governed by interactions between the electron-donating porphyrin and the electron-accepting fullerene. Importantly, positive cooperativity between the applied binding motifs is corroborated by a number of experimental techniques, such as NMR, absorption, fluorescence, etc. In addition, transient absorption experiments shed light onto electron-transfer processes taking place in the ground state and upon photoexcitation. In fact, porphyrin excitation powers an electron transfer to the fullerene yielding charge separated state lifetimes in the nanosecond regime.

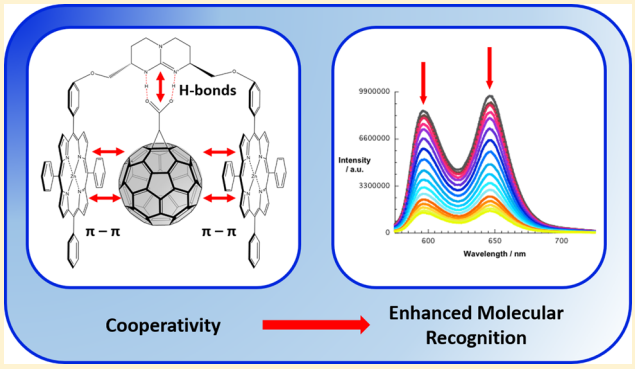

INTRODUCTION

In light of the world's demand regarding renewable energy sources, solar energy, in general, and organic photovoltaics, in particular, have emerged as key players in recent decades.[1] Great abundance and low production costs are just a few of the numerous incentives that organic photovoltaics feature over conventional techniques, such as silicon-based solar cells. Importantly, concerted efforts have been directed to develop molecular systems for the mimicry of natural photosynthesis.[2] In particular, cascades of light induced energy and electron-transfer reactions assist in harvesting light and converting it into free charge carriers, that is, electrons and holes. An essential requirement for them to function effectively is the hierarchical organization of the molecular building blocks by, for example, noncovalent motifs.[3] Leading examples are hydrogen-bonding, $\pi-\pi$-interactions, n-π-interactions etc. On one hand, porphyrinoids have been widely employed as light harvester/electron donor, owing to their favorable character as natural chromophores and panchromatic light harvester.[4] On the other hand, fullerenes have revealed themselves as an electron accepting complement to porphyrins.[5] The rigid and well confined structure of fullerenes renders them perfectly suitable for single and multi electron-transfer reactions in, for example, artificial photosynthetic reaction centers.[6]

In light of the aforementioned, the combination of fullerenes and porphyrins in the form of electron donor–acceptor conjugates and hybrids have evolved into a thoroughly studied field of research.[7] As a matter of fact, electron-transfer processes in terms of charge separation and charge recombination between electron donating porphyrins and electron accepting fullerenes have been elucidated and many similarities relative to the natural photosynthetic systems have been established.[8] In terms of noncovalent hybrids, viable strategies consist of a careful design of porphyrin based receptors, which strongly bind fullerene guests, and, which result in the assembly of stable and robust architectures.[9]

We previously reported the synthesis and the study of stable supramolecular electron donor–acceptor hybrids with unique photophysical features.[10] Our approach consisted of assembling electron accepting C_{60} derivatives with the electron donor tetrathiafulvalene (TTF) through complementary guanidinium–carboxylate interactions. From a full fledged spectroscopic characterization formation of the charge separated radical ion pair states $C_{60}^{\bullet-}$·$TTF^{\bullet+}$ was inferred. The latter features lifetimes in the range of hundreds of nanoseconds. As such, the flexibility of the system and the spatial proximity between the electron donor and the electron acceptor via noncovalent interactions enable unidirectional and efficient through space electron-transfer interactions.

En-route towards establishing hydrogen-bonding based supramolecular electron donor–acceptor hybrids we describe herein the synthesis and properties of guanidinium bis-porphyrin tweezers **1**, which has been specifically designed to

Received: May 25, 2014
Published: July 11, 2014

   dx.doi.org/10.1021/ja5052236 | J. Am. Chem. Soc. 2014, 136, 11436–11443

interact with (1,2-methanofullerene C_{60})-61-carboxylate salt **3** (Figure 1). Past studies have documented that tweezers like

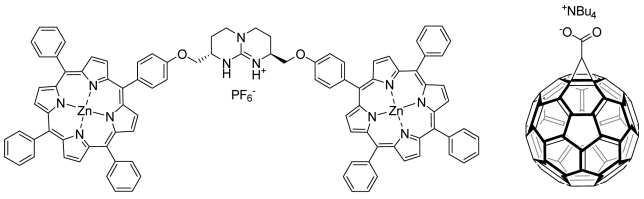

Figure 1. Guanidinium bis-porphyrin tweezers **1** and fullerene carboxylate **3**.

geometries are a sound platform for efficient supramolecular binding.[11] Additional $\pi-\pi$ interactions as they play a significant role between porphyrins and fullerenes, in general, should further strengthen the overall binding.[12] Bicyclic guanidiniums bind a wide variety of anions, especially oxoanions, due to the creation of well oriented hydrogen-bonded ion pairs.[13] Thus, the guanidinium scaffold not only acts as a structural linker between the two porphyrins, but it also plays an active role to complement anionic guests. In fact, fullerene carboxylate **3** is expected to match nicely the geometrical and electronic requirements of bis-porphyrin tweezers **1** and to form **3@1**. We will demonstrate that the assembly of **1** and **3** is characterized by an unprecedented high binding strength and electron-transfer activity once photoexcited. Most importantly, the contribution of each binding motif will be determined by comparison with suitable models to allow estimating their cooperativity and their impact on the rates and yields of electron transfer.

RESULTS AND DISCUSSION

Design of Guanidinium Bis-porphyrin Tweezers. The choice of the spacer and binding motif between the guanidinium scaffold and the porphyrin moieties was evaluated by molecular modeling. The short ether linkage fits nicely with the geometrical and spatial requirements to form a complex with C_{60}. Longer spacers would increase the distance between the porphyrin planes as well as with the bicyclic guanidinium scaffold and, in turn, disfavor binding of fullerene carboxylate **3**. Indeed, subtle structural considerations are essential for the design of this receptor.

For instance, *p*-phenoxy-porphyrins enable the correct geometry for C_{60} complexation. As shown in Figure 2, the molecular model of **3@1** implies that the porphyrin planes are at a 12.2 Å distance relative to each other with a parallel

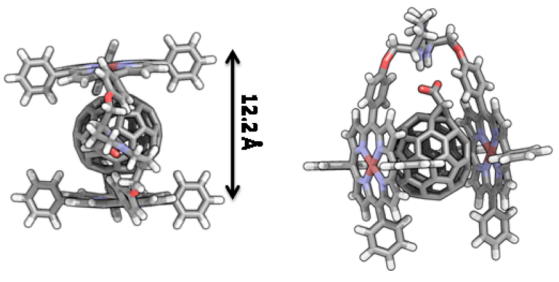

Figure 2. Optimized structure (SCIGRESS, standard conditions, no solvent) of **3@1** in top view (left) and front view (right); Zn/C_{60} distance is ca. 3.2 Å.

orientation and, in turn, induce the right fitting with respect to C_{60}. From the analysis of 21 C_{60}@ZnP cocrystal structures taken from the Cambridge Structural database, the average distances between the centroids of the ZnP planes and C_{60} is 6.28 ± 0.08 Å. This value is consistent with that calculated for **3@1**. For a *meta*-substitution, the distances between porphyrins in parallel disposition would be larger than 14 Å, and therefore, the porphyrins would need to bend in order to provide the proper geometry for hosting C_{60}. Another consideration about *meta*-substituted (m-phenoxy) porphyrins is their relative close distance to the guanidinium scaffold, which would hamper a suitable orientation and/or distance to form simultaneously the salt bridge with the carboxylate and the corresponding $\pi-$electron interactions with C_{60}.

Nevertheless, the acyclic tweezers **1** is highly adaptable, since the porphyrins are only tethered from one side. Binding fullerene carboxylate **3** should, however, restrict the overall conformation of the molecule to a parallel orientation of the two porphyrins as shown in the molecular models.

Synthesis of Guanidinium Bis-Porphyrin Tweezers. Guanidinium bis-porphyrin tweezers **1** was prepared by O-alkylation of Zn-*meso*-5-(4′-hydroxyphenyl)-10,15,20-triphenyl-porphyrin (**4**)[14] with guanidinium salt **5** in 42% yield. Previous zinc metalation of the porphyrin is necessary in order to avoid the undesired N-alkylation of the porphyrin nitrogens (Scheme 1).

Scheme 1. Synthesis of Guanidinium Bis-Porphyrin Tweezers 1[a]

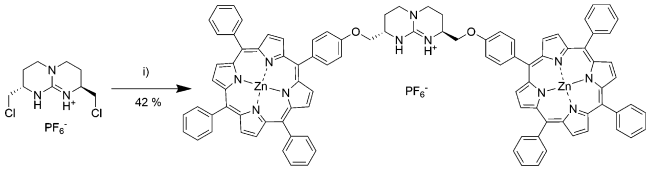

[a]Conditions: (i) 2.2 equiv of **4**, 4.5 equiv K_2CO_3, acetone, reflux.

For solubility reasons, the tetrabutylammonium fullerene carboxylate salt **3** was prepared by addition of equimolar amounts of tetrabutylammonium hydroxide to a solution of commercially available (1,2-methanofullerene C_{60})-61-carboxylic acid in *ortho*-dichlorobenzene.

Guanidinium hexafluorophosphate salt **2** was prepared as a control to dissect the contribution of the guanidinium-carboxylate to the overall binding with **1**. Synthesis of **2** was achieved as previously described by O-alkylation of phenol with guanidinium salt **5**, see Scheme 2. Details are presented in the Experimental Section, Supporting Information.

Finally, guanidinium monoporphyrin **6** was synthesized as a reference to gather insights into the thermodynamics of the association, including the determination of the effective

Scheme 2. Synthesis of Bis-Aryl Guanidinium Hexafluorophosphate Salt 2[a]

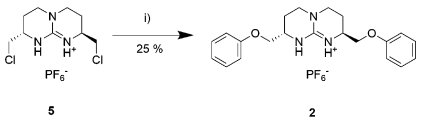

[a]Conditions: (i) 2.9 equiv of phenol, 5 equiv K_2CO_3, acetone, reflux.

dx.doi.org/10.1021/ja5052236 | J. Am. Chem. Soc. 2014, 136, 11436−11443

molarity (EM) and the assessment of the cooperativity. Following the methodology depicted above, O-alkylation of Zn-phenolporphyrin **4** with monoprotected guanidine **7**[15] afforded compound **6** in good yields (Scheme 3).

Scheme 3. Synthesis of Guanidinium Mono-Porphyrin 6[a]

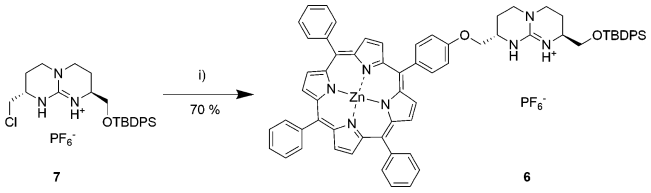

[a]Conditions (i) 1.5 eq of **7**, 1 equiv of **4**, 1.5 equiv K_2CO_3, acetone, reflux.

Complexation Studies of Bis-Porphyrin Tweezers 1 with C_{60} and Fullerene Carboxylate 3. To evaluate the binding motif and the association constants for **1** with C_{60} and with fullerene carboxylate **3** to afford **C_{60}@1** and **3@1**, respectively, ^{1}H NMR experiments were performed. Only minor changes were observed upon addition of C_{60} to the guanidinium bis-porpyhrin tweezers **1** in deuterated toluene (Figure S1).

Please note that C_{60} has a unique ^{13}C signal due to the equivalence of all its carbons. Indeed, the ^{13}C NMR spectrum of **C_{60}@1** in tetrachloroethane revealed a rather significant upfield shift of the C_{60} signal. A likely rationale for the upshift is an effective complexation of C_{60} as previously reported by Boyd et al.[11e] As such, complexation results in a chemical shift as an average signal corresponding to free/uncomplexed and complexed C_{60}, see Figure 3. Upon heating, the stability of

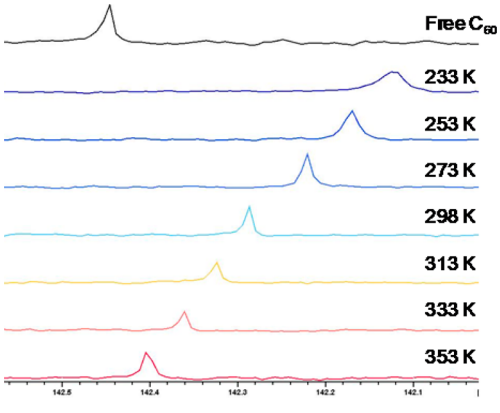

Figure 3. ^{13}C NMR spectra in TCE-d_2 of C_{60} (top) and **C_{60}@1** at different temperatures.

C_{60}@1 decreases, and the signal shifts toward the resonance seen for free/uncomplexed C_{60}. Upon cooling, the association process becomes more favorable. We were, however, unable to reach the coalescence temperature, that is, the point at which the equilibrium between free/uncomplexed and complexed C_{60} is slow enough to discern both signals.

C_{60}@1 was further characterized by mass spectrometry revealing in ESI an isotopically enriched ion of 2273.5 m/z relative to 1552.4 m/z for just the bis-porphyrin tweezers **1**. As gathered in Figure 4, the experimental and the calculated isotopic patterns are in good agreement with each other.

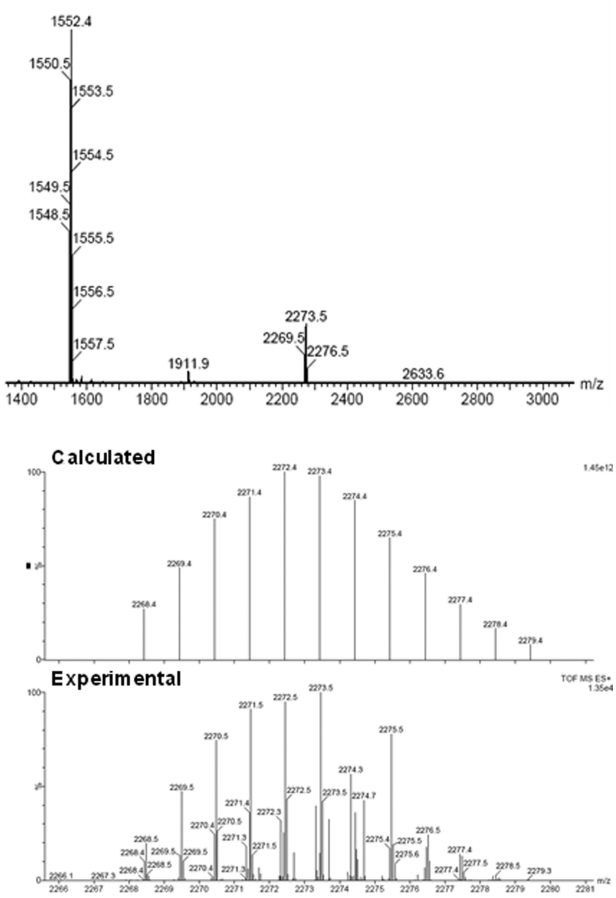

Figure 4. Upper part: Mass spectrum of **C_{60}@1**. Lower part: Calculated and experimental isotopic pattern of **C_{60}@1**.

In addition, ^{1}H NMR titrations were performed with fullerene carboxylate **3** and tweezers **1**. As in the case of C_{60}, the ^{1}H NMR spectra gave rise to minor chemical shifts when *ortho*-dichlorobenzene was used as a solvent, see Figure 5.

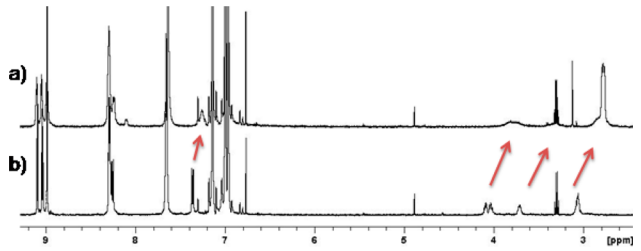

Figure 5. ^{1}H NMR spectra in *ortho*-dichlorobenzene-d_4 of guanidinium bis-porphyrin tweezers **1** in the presence (1 equiv) (a) and the absence (b) of fullerene carboxylate **3**.

Upfield shifts of the guanidinium protons are taken as evidence for structural rearrangements of the flexible guanidinium scaffold that induces maximum interactions with fullerene carboxylate **3** in **3@1**. It is interesting to note that the aromatic protons in the *ortho* positions of the phenoxy moieties also showed both upfield shifts and broadening. Moreover, the formation of complex **3@1** was corroborated in mass spectrometric experiments, MALDI, with a M^+ of 2330 m/z (Figure S2).

Finally, titrations of model receptor **2** with fullerene carboxylate **3** were performed in chlorobenzene-d_5, and the

dx.doi.org/10.1021/ja5052236 | J. Am. Chem. Soc. 2014, 136, 11436−11443

corresponding ^{1}H NMR spectra were used to assess the contribution of the guanidinium-carboxylate salt bridge to the overall binding. From Figure 6, which illustrates the downfield

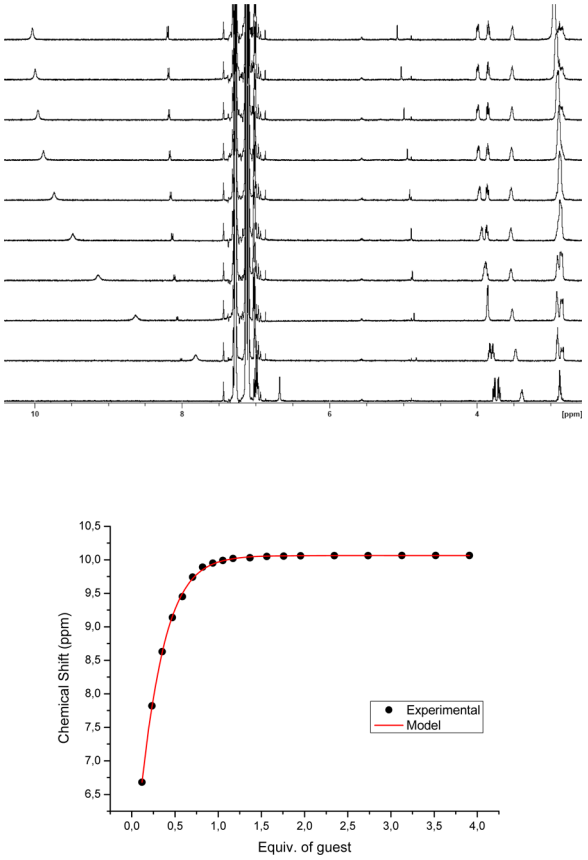

Figure 6. Upper part: ^{1}H NMR titration in chlorobenzene-d_5 of model guanidinium salt **2** with fullerene carboxylate **3**. Lower part: plot of the chemical shift of the guanidinium protons vs equivalents of **3** added.

shift of the guanidinium protons upon complexation, an association constant of 3.3×10^3 M^{-1} was derived for **3@2**. This value is in sound agreement with the association constants determined for similar guanidinium-carboxylate systems in nonpolar media.[16]

In summary, ^{1}H NMR studies and mass spectrometry analysis of the complexes confirmed that sizable interactions of C_{60} and fullerene carboxylate guest **3** with bis-porphyrin tweezers **1** are the inception to form a rather strong complex, namely C_{60}**@1**. By means of variable-temperature ^{13}C NMR studies the encapsulation of C_{60} by guanidinium bis-porphyrin tweezers **1** was further demonstrated. The nature of this complexation relies on the electronic complementarity between the electron-donating porphyrin tweezers **1** and the electron-accepting fullerene. With the fullerene carboxylate **3**, the higher chemical shifts corresponded to the guanidinium scaffold protons. This prompts to a structural rearrangement of the flexible backbone to properly adapt and dock with **3**.

Photophysical Studies of Bis-Porphyrin Tweezers 1 with C_{60} and Fullerene Carboxylate 3. To gain further insights into supramolecular ground-state interactions between **1** and **3** in solution, absorption assays were carried out. To this end, **3** was added stepwise to a solution containing a constant concentration of **1** in *ortho*-dichlorobenzene to reach molar ratios of 5:1 between **3** and **1**. With increasing concentration of **3**, the ZnP Soret band at 425 nm undergoes a slight red shift and a lowering in intensity, see Figure 7.

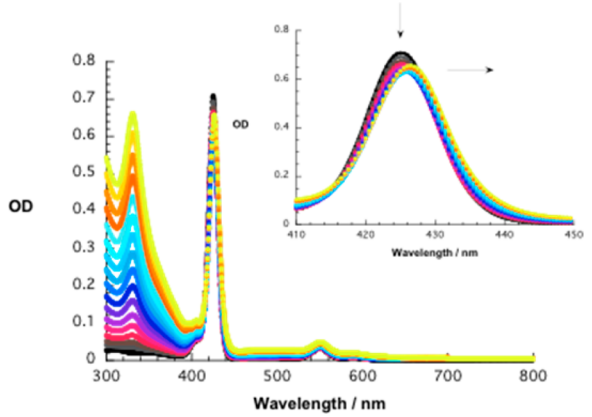

Figure 7. Absorption spectra of a dilute *ortho*-dichlorobenzene solution of **1** (9.0×10^{-7} M) in the presence of variable concentrations of **3** (0; 1.9×10^{-7}, 3.7×10^{-7}, 6.5×10^{-7}, 1.0×10^{-6}, 1.4×10^{-6}, 1.9×10^{-6}, 2.4×10^{-6}, 3.0×10^{-6}, 4.2×10^{-6}, 4.8×10^{-6}, 5.5×10^{-6}, 6.2×10^{-6}, 7.5×10^{-6}, 8.3×10^{-6} M). Arrows indicate the progression of the titration.

Importantly, addition of **2**, a reference bearing the same hydrogen-bonding motif present in **1** but lacking ZnP, the original ZnP Soret peak intensity and position is recovered, see Figure S3. In other words, **1** is successfully replaced in **3@1** by **2** to afford **3@2**. In an extra set of titrations, an equimolar mixture of **2** and **3** was added to **1**. Again, a red shift and a lowered intensity of the ZnP Soret band are observed. Based on the aforementioned titrations we conclude that rather strong interactions power the formation of **3@1**. It is safe to assume that positive cooperativity made out of hydrogen bonding and $\pi-\pi$ interactions prevail between guanidinium bis-porphyrin tweezers **1** and fullerene carboxylate **3**, *vide infra*.

Complementary titrations of **1** with C_{60} revealed lowered Soret band intensity in the presence of C_{60} but no appreciable red shift. Notable is the necessity to employ much higher C_{60} concentrations relative to **3** in order to induce the lowering in Soret band intensity.

To shed light onto the excited-state interactions between **1**, on one hand, and **3** or C_{60}, on the other hand, fluorescence titrations were carried out. Here, upon addition of **3** (Figure 8) or C_{60} (Figure S4) to a solution of **1** in *ortho*-dichlorobenzene, a nearly quantitative quenching of the ZnP fluorescence evolves when exciting at 419 and 416 nm, respectively, as a consequence of forming **3@1** and C_{60}**@1**. Like in the absorption experiments, addition of **2** to **3@1** led to a quantitative recovery of the ZnP fluorescence, see Figure S5. The overall fluorescence quenching within the concentration range from 10^{-7} to 10^{-5} M was much more pronounced for **3** when compared with C_{60}, see Figure S4.

To quantify the binding strength, the intensity of the ZnP fluorescence at 646 nm was plotted versus the concentration of either **3** or C_{60}. Nonlinear curve fitting allowed calculating the association constants (K_a). The resulting K_a values were 3×10^3 and 2.3×10^6 M^{-1} for C_{60} and **3**, respectively. We assign the rather significant difference of 3 orders of magnitude to the cooperativity stemming from $\pi-\pi$ interactions and hydrogen-bonding interactions in the case of **3**. In line with the expectation, the corresponding association constant for the

dx.doi.org/10.1021/ja5052236 | J. Am. Chem. Soc. 2014, 136, 11436−11443

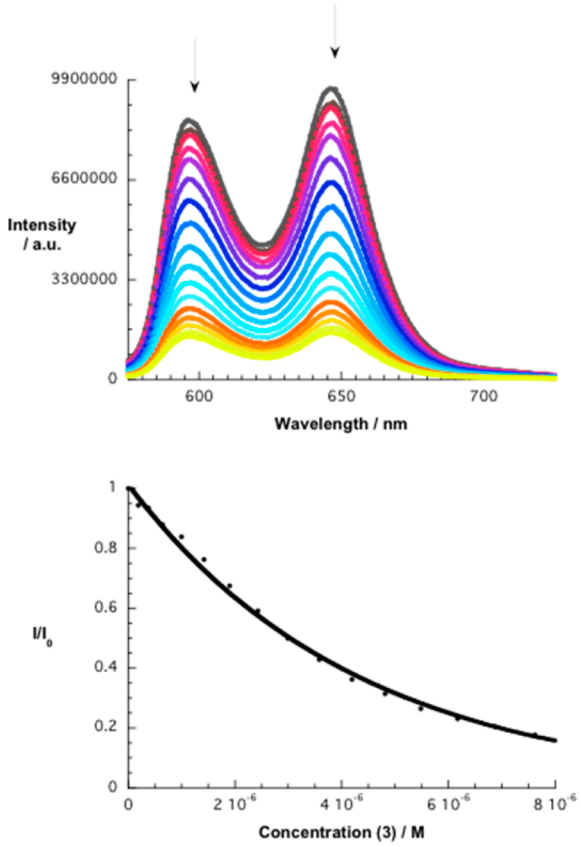

Figure 8. Upper part: fluorescence spectra upon 419 nm excitation of a dilute *ortho*-dichlorobenzene solution of **1** (9.0×10^{-7} M) in the presence of variable concentrations of **3** (0; 1.9×10^{-7}, 3.7×10^{-7}, 6.5×10^{-7}, 1.0×10^{-6}, 1.4×10^{-6}, 1.9×10^{-6}, 2.4×10^{-6}, 3.0×10^{-6}, 4.2×10^{-6}, 4.8×10^{-6}, 5.5×10^{-6}, 6.2×10^{-6}, 7.5×10^{-6}, 8.3×10^{-6} M). Arrows indicate the progression of the titration. Lower part: plot of I/I_0 for the fluorescence of **1** observed at 646 nm vs concentration of **3**.

formation of **3@2**, which is exclusively built on hydrogen bonding, is notably weaker with a value of 3.3×10^3 M^{-1} that was determined by NMR titration. In a titration of monoporphyrin **6** with **3**, a binding constant of 1.1×10^6 M^{-1} was determined. Taking the aforementioned into context, the differences between **3@1**, **C_{60}@1**, **3@6**, and **3@2** unambiguously corroborate the positive cooperativity, *vide infra*.

Analyses of the Equilibria of Bis-Porphyrin Tweezers 1 with C_{60} and Fullerene Carboxylate 3. With these data in hand, the contribution of each individual interaction and the possible cooperativity effects arising from these multivalent systems can be analyzed. For the formation of **3@1**, we should consider four different equilibria, as depicted in Scheme 4. Please note that the order by which the different equilibria are considered should not alter the overall binding. Hence, initially guanidinium-carboxylate pairing takes place (K_1) followed by the intramolecular (EM_1) binding of one of the two ZnPs (K_2). Successive intramolecular (EM_2) binding of the second ZnP (K_2) leads to the formation of **3@1**.

By definition, the cooperativity factor (α) is the ratio between the experimental association constant, which is affected by cooperative interactions (K_A), and the statistical or the reference constant (K_{ref}).[17] As the association constant and the reference constant have the same value in the absence of cooperativity, a consistent cooperativity factor should be close to 1, while positive or negative cooperativity leads to $\alpha > 1$ or $\alpha < 1$, respectively. In the current case, cooperativity, which stems from a chelation effect, needs to be considered as two or more intramolecular binding interactions interplay collectively. However, chelate cooperativity depends on ligand concentrations. For simplicity, we consider from now on eq 1.

$$\alpha = \frac{K_A}{K_{ref}} \tag{1}$$

Taking a binding constant K_2 for C_{60}/ZnP interactions in toluene of 3×10^3 M^{-1} into account,[18] we are able to

Scheme 4. Thermodynamic Equilibrium Processes Involving the Complexation of Fullerene-Carboxylate 3 with Bis-Porphyrin Tweezers 1

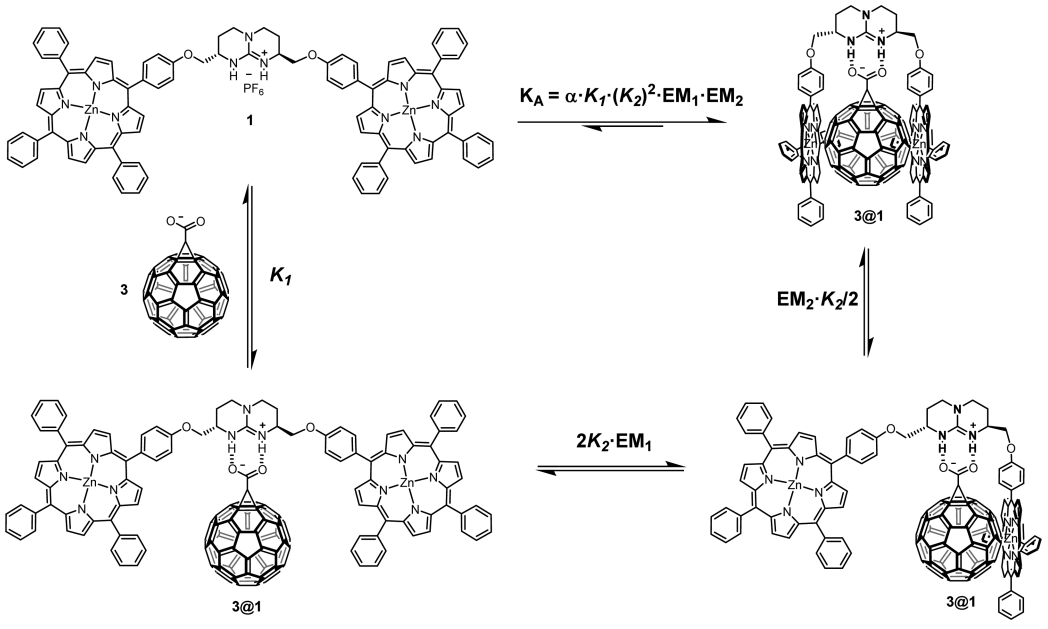

dx.doi.org/10.1021/ja5052236 | J. Am. Chem. Soc. 2014, 136, 11436−11443

extrapolate the effective molarities, namely EM_1 and EM_2, from the stability constant values of **3@6** and **C_{60}@1**, respectively. These data allow us to estimate a reference constant for this system. The reference constant is the expected theoretical constant − the sum of all contributions from the different interactions in a multivalent system, neglecting any cooperativity between those interactions. In our case, we estimate the reference constant, as different experimental techniques were employed (NMR, UV−vis absorption/emission). The latter is kept constant as the denominator for deriving the cooperativity factor. For the numerator we use the experimentally determined stability constant for **3@1**.

Scheme 5 depicts the equilibria for the complexation between guanidinium monoporphyrin **6** and fullerene carboxylate **3** with K_B of 1.1×10^6 M^{-1}, see Figure S6, which are employed to determine the effective molarity (EM_1) needed to describe the cooperativity between bis-porphyrin **1** and fullerene carboxylate **3**.

Scheme 5. Thermodynamic Equilibrium Processes Involving the Complexation of Fullerene-Carboxylate 3 with Mono-Porphyrin Compound 6

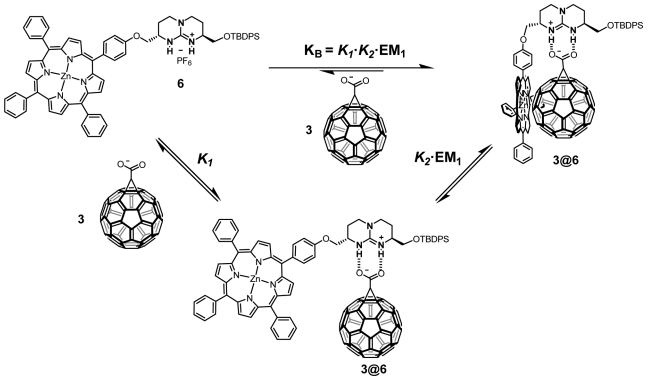

Notable, the guanidinium-carboxylate stability constant K_1 is taken as 3.3×10^3 M^{-1} from the titrations of guanidinium salt **2** with fullerene carboxylate **3**. Using the above-mentioned K_2, we calculated an EM_1 value of 0.1 M. Likewise, by using the experimental association constant K_C regarding the complexation between **1** and **C_{60}** as 4.7×10^3 M^{-1} (Scheme 6), we determined an EM_2 value of 5×10^{-4} M.

With these data in hand, we estimated K_{ref} as 1.5×10^6 M^{-1}. Dividing the experimental stability constant K_A (for **3@1**, 2.3×10^6 M^{-1}) by K_{ref} afforded a cooperativity factor of $\alpha \approx 2$. This suggests that positive cooperativity governs the interactions and, in turn, enhances the thermodynamic stability of **3@1**. To facilitate the overall interpretation, we have dismissed side-processes, such as self-aggregation, higher complex stoichiometries, etc., which may impact the different equilibria.

Scheme 6. Thermodynamic Equilibrium Processes Involving the Complexation of C_{60} with Guanidinium Bis-Porphyrin 1

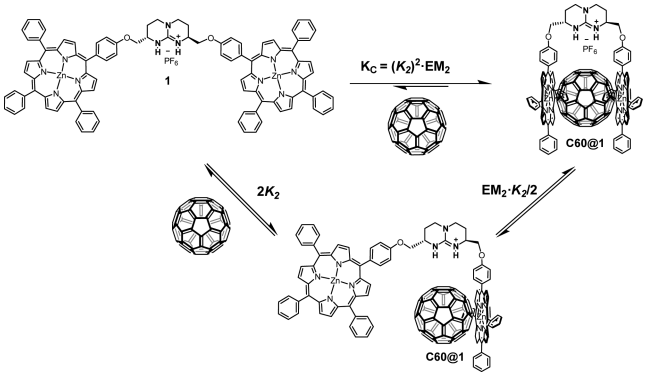

To shed light onto the influence of ionic strength on the equilibrium, additional titration experiments using absorbance and fluorescence were conducted. Therefore, addition of various ratios of NaOH (5×10^{-4} M in 2-propanol) was probed, and the binding constants increased to 8.1×10^6 M^{-1} for a 1:1 ratio of NaOH and **1**, see Figure S7. Notably, the binding constant maximizes at a 1:1 stoichiometric ratio and decreases upon further increasing the ratio. This 4-fold increase of the binding constant meets the expectations, as NaOH facilitates the solvation of the guanidinium cations and the corresponding counteranions. At NaOH concentrations larger than the concentration of **1**, higher ionic strengths impact the binding constant.

To conclude, we have demonstrated the formation of a stable and robust C_{60}/ZnP electron donor−acceptor hybrid, which is based not only on electronic complementarity but also on hydrogen-bonding and electrostatic interactions between the bicyclic guanidinium scaffold and the carboxylate moiety of C_{60}.

Electron-Transfer Studies of Bis-Porphyrin Tweezers 1 with C_{60} and Fullerene Carboxylate 3. Insights into excited-state interactions between **1** and **3** or **C_{60}** were gathered from femtosecond transient absorption spectroscopy. 150 fs laser pulses were used to probe **3@1** and **C_{60}@1**. When **1** was subjected to 420 nm pulses in *ortho*-dichlorobenzene transients were observed immediately after the laser pulse that are characteristical for ZnP singlet excited states, see Figure S8.[19] In particular, a broad transient with a maximum around 460 nm, a minimum at 550 nm, and several weaker maxima between 570 and 750 nm is assigned to singlet−singlet transitions involving the ZnP singlet excited state. The singlet state relaxes via intersystem crossing within 0.9 ns to the corresponding triplet state. Such a singlet excited-state lifetime is shorter than the lifetime known for ZnP monomers (~2.0 ns). A reasonable rationale for these data involves electronic communication between the two ZnPs present in **1**.

When exciting equimolar mixtures of **1** and **3**, presumably **3@1**, in *ortho*-dichlorobenzene or toluene at 420 nm the same ZnP singlet excited-state features develop that were seen in experiments with **1**, *vide supra*. However, the ZnP singlet excited-state decay in **3@1** is faster and is of a different nature when compared to photoexcited **1**. In particular, transient features in the visible range of the spectrum, that is, from 600 to 800 nm, and in the near-infrared range of the spectrum, that is, from 800 to 1050 nm, appear. The earlier band bears great resemblance with the one-electron oxidized form of ZnP,[20] while the latter band bears great resemblance with the one-electron reduced form of C_{60}.[21] We assign the overall features to the radical ion pair state of **3@1**, that is, **$3^{\bullet-}$@$1^{\bullet+}$**. Similar observations were made in toluene, see Figure S9. On the contrary, 420 nm excitation in THF failed to yield any evidence for **$3^{\bullet-}$@$1^{\bullet+}$**, see Figure S10. A possible rationale is that THF competes with **3** in terms of hydrogen bonding and, in turn, decreases the association constant.

When investigating the charge recombination dynamics by means of multiwavelength analyses, lifetimes of 2.1 and 1.3 ns for the **$3^{\bullet-}$@$1^{\bullet+}$** radical ion pair state were derived in toluene and *ortho*-dichlorobenzene, respectively. The longer radical ion

dx.doi.org/10.1021/ja5052236 | J. Am. Chem. Soc. 2014, 136, 11436−11443

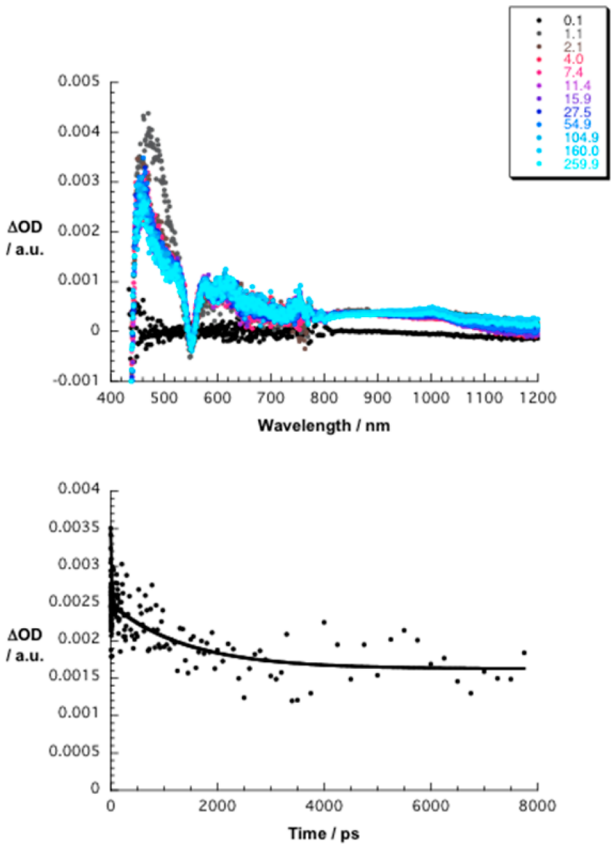

Figure 9. Upper part: differential absorption spectra (visible and near-infrared) obtained upon femtosecond flash photolysis (420 nm) of a 1:1 mixture of **1** and **3** in Ar-saturated *ortho*-dichlorobenzene with time delays between 0.1 and 260 ps at room temperature. Lower part: time-absorption profile at 460 nm, reflecting the charge separation and charge recombination.

pair state lifetime in toluene relates to the lower solvent polarity of toluene when compared to *ortho*-dichlorobenzene as a means to push the corresponding kinetics into the Marcus inverted region.[22]

Equimolar mixtures of **1** and C_{60}, either in toluene, *ortho*-dichlorobenzene, or THF, which were subjected to 420 nm excitation did not result in any noticeable charge-transfer activity. A reasonable rationale is the weak association constant for **C_{60}@1** when compared to **3@1**. Thus, the concentration of C_{60} was increased to reach a molar ratio of 10:1, and in fact, weak features of $C_{60}^{\bullet-}$ and $\mathbf{1}^{\bullet+}$ are discernible. For $C_{60}^{\bullet-}$**@1**$^{\bullet+}$, kinetic analysis of the charge recombination dynamics revealed radical ion pair state lifetimes of 0.7, 1.1, and 1.8 ns in toluene, *ortho*-dichlorobenzene, and THF, respectively.

CONCLUSION

In summary, a novel supramolecular electron donor–acceptor hybrid **3@1** has been assembled and characterized. The cooperativity between π–π stacking and hydrogen bonding has been demonstrated to result in strong binding. In fact, the additional hydrogen bonding increases the association constant from 10^3 to 10^6 M^{-1} for **C_{60}@1** and **3@1**, respectively. Equally important is the fact that excitation of **C_{60}@1** and **3@1** generates a nanosecond-lived radical ion pair state.

ASSOCIATED CONTENT

Supporting Information

Synthetic procedures and characterization and additional photochemical data. This material is available free of charge via the Internet at http://pubs.acs.org.

AUTHOR INFORMATION

Corresponding Author

dirk.guldi@fau.de

Present Address

[‖]LIMES Institute, Chemical Biology and Medicinal Chemistry Unit, c/o Kekulé Institute of Organic Chemistry and Biochemistry, Gerhard-Domagk-Strasse 1, 53121 Bonn, Germany.

Author Contributions

[‡]These authors contributed equally.

Notes

The authors declare no competing financial interest.

ACKNOWLEDGMENTS

The authors thank the Deutsche Forschungsgemeinschaft and the Bavarian Initiative – Solartechnologies Go Hybrid for generous funding of this work. Dedicated to Prof. Tim Clark on the occasion of his 65th birthday.

REFERENCES

(1) (a) Eisenberg, R.; Nocera, D. G. *Inorg. Chem.* **2005**, *44*, 6799–6801. (b) Wengenmair, R.; Bührke, T. *Renewable Energy: Sustainable Energy Concepts for the Future*; Wiley: Weinheim, Germany, 2008.

(2) (a) Collings, A. F.; Critchley, C. *Artificial Photosynthesis: From Basic Biology to Industrial Applications*; Wiley, Weinheim, Germany, 2005. (b) Sundstrom, V. *Solar Energy Conversion - Natural to Artificial*; Springer: Dordrecht, TheNetherlands, 2009.

(3) (a) Blankenship, R. E. *Molecular Mechanism of Photosynthesis*; Blackwell: Oxford, 2002. (b) Alberts, B. *Molecular Biology of the Cell*; Garland: New York, 2008. (c) Green, B. R.; Parson, W. W. *Light-Harvesting Antennas in Photosynthesis*; Kluwer: Dordrecht, The Netherlands, 2003. (d) McEvoy, J. P.; Brudvig, G. W. *Chem. Rev.* **2006**, *106*, 4455–4483. (e) Fukuzumi, S. *Phys. Chem. Chem. Phys.* **2008**, *10*, 2283–2297.

(4) (a) Taniguchi, M.; Lindsey, J. S. *Tetrahedron* **2010**, *66*, 5549–5565. (b) Lee, C. Y.; Jang, J. K.; Kim, C. H.; Jung, J.; Park, B. K.; Park, J.; Choi, W.; Han, Y.-K.; Joo, T.; Park, J. T. *Chem.—Eur. J.* **2010**, *16*, 5586–5599. (c) Moore, G. F.; Hambourger, M.; Gervaldo, M.; Poluektov, O. G.; Rajh, T.; Gust, D.; Moore, T. A.; Moore, A. L. *J. Am. Chem. Soc.* **2008**, *130*, 10466–10467. (d) Kelley, R. F.; Lee, S. J.; Wilson, T. M.; Nakamura, Y.; Tiede, D. M.; Osuka, A.; Hupp, J. T.; Wasielewski, M. R. *J. Am. Chem. Soc.* **2008**, *130*, 4277–4284. (e) Nakamura, Y.; Aratani, N.; Osuka, A. *Chem. Soc. Rev.* **2007**, *36*, 831–845. (f) Satake, A.; Kobuke, Y. *Org. Biomol. Chem.* **2007**, *5*, 1679–1691. (g) Gadde, S.; Shafiquil Islam, D.-M.; Wijesinghe, C. A.; Subbaiyan, N. K.; Zandler, M. E.; Araki, Y.; Ito, O.; D'Souza, F. *J. Phys. Chem. C* **2007**, *111*, 12500–12503. (h) Langford, S. J.; Latter, M. J.; Woodward, C. P. *J. Photochem. Photobiol.* **2006**, *82*, 1530–1540. (i) Prodi, A.; Chiorboli, C.; Scandola, F.; Iengo, E.; Alessio, E.; Dobrawa, R.; Würthner, F. *J. Am. Chem. Soc.* **2005**, *127*, 1454–1462. (j) Imahori, H.; Mori, Y.; Matano, Y. *J. Photochem. Photobiol., C* **2003**, *4*, 51–83. (k) Armaroli, N.; Marconi, G.; Echegoyen, L.; Bourgeois, J.-P.; Diederich, F. *Chem.—Eur. J.* **2000**, *6*, 1629–1645. (l) Kurreck, H.; Huber, M. *Angew. Chem., Int. Ed. Engl.* **1995**, *34*, 849–866. (m) Wasielewski, M. R. *Chem. Rev.* **1992**, *92*, 435–461. (n) Guldi, D. M. *J. Phys. Chem. B* **2005**, *109*, 11432–11441. (o) Imahori, H.; Guldi, D. M.; Tamaki, K.; Yoshida, Y.; Luo, C.; Sakata, Y.; Fukuzumi, S. *J. Am. Chem. Soc.* **2001**, *123*, 6617–6628. (p) D'Souza, F.; Ito, O. *Chem. Commun.* **2009**, *33*, 4913–4928. (q) Takai, A.; Chkounda, M.;

Eggenspiller, A.; Gros, C. P.; Lachkar, M.; Barbe, J.-M.; Fukuzumi, S. *J. Am. Chem. Soc.* **2010**, *132*, 4477−4489.
(5) Hirsch, A.; Brettreich, M. *Fullerenes: Chemistry and Reactions*; Wiley: Weinheim, Germany, 2005.
(6) (a) El-Khouly, M. E.; Kim, J. H.; Kay, K.-Y.; Choi, C. S.; Ito, O.; Fukuzumi, S. *Chem.—Eur. J.* **2009**, *15*, 5301−5310. (b) Rio, Y.; Seitz, W.; Gouloumis, A.; Vázquez, P.; Sessler, J. L.; Guldi, D. M.; Torres, T. *Chem.—Eur. J.* **2010**, *16*, 1929−1940.
(7) (a) Guldi, D. M. *Chem. Commun.* **2000**, *5*, 321−327. (b) Sun, D.; Tham, F. S.; Reed, C. A.; Boyd, P. D. W. *Proc. Natl. Acad. Sci. U.S.A.* **2002**, *99*, 5088−5092. (c) Guldi, D. M. *Chem. Soc. Rev.* **2002**, *31*, 22−36. (d) Boyd, P. D. W.; Reed, C. A. *Acc. Chem. Res.* **2005**, *38*, 235−242. (e) Tashiro, K.; Aida, T. *Chem. Soc. Rev.* **2007**, *36*, 189−197.
(8) (a) Gust, D.; Moore, T. A.; Moore, A. L. *Acc. Chem. Res.* **2001**, *34*, 40−48. (b) Imahori, H.; Fukuzumi, S. *Adv. Funct. Mater.* **2004**, *14*, 525−536.
(9) (a) Yanagisawa, M.; Tashiro, K.; Yamasaki, M.; Aida, T. *J. Am. Chem. Soc.* **2007**, *120*, 11012−11013. (b) Schmittel, M.; He, B.; Mal, P. *Org. Lett.* **2008**, *10*, 2513−2516. (c) Tashiro, K.; Aida, T.; Zheng, J.-Y.; Kinbara, K.; Saigo, K.; Sakamoto, S.; Yamaguchi, K. *J. Am. Chem. Soc.* **1999**, *121*, 9477−9478. (d) D'Souza, F.; Chitta, R.; Gadde, S.; Zandler, M. E.; McCarty, A. L.; Sandanayaka, A. S. D.; Araki, Y.; Ito, O. *Chem.—Eur. J.* **2005**, *11*, 4416−4428. (e) D'Souza, F.; Gadde, S.; Zandler, M. E.; Itou, M.; Araki, Y.; Ito, O. *Chem. Commun.* **2004**, 2276−2277. (f) D'Souza, F.; Chitta, R.; Gadde, S.; Zandler, M. E.; Sandanayaka, A. S. D.; Araki, Y.; Ito, O. *Chem. Commun.* **2005**, 1279−1281. (g) Tashiro, K.; Aida, T. *Chem. Soc. Rev.* **2007**, *36*, 189−197. (h) Yamaguchi, T.; Ishii, N.; Tashiro, K.; Aida, T. *J. Am. Chem. Soc.* **2003**, *125*, 13034−13035.
(10) Segura, M.; Sanchez, L.; de Mendoza, J.; Martin, N.; Guldi, D. M. *J. Am. Chem. Soc.* **2003**, *125*, 15093−15100.
(11) (a) Fathalla, M.; Jayawickramarajah, J. *Eur. J. Org. Chem.* **2009**, *35*, 6095−6099. (b) Pérez, E. M.; Martín, N. *Pure Appl. Chem.* **2010**, *82*, 523−533. (c) Torres, T.; Bottari, G. *Organic Nanomaterials*; Wiley: Hoboken, NJ, 2013. (d) Grimm, B.; Santos, J.; Illescas, B. M.; Muñoz, A.; Guldi, D. M.; Martín, N. *J. Am. Chem. Soc.* **2010**, *132*, 17387−17389. (e) Sun, D.; Tham, F. S.; Reed, C. A.; Chaker, L.; Burgess, M.; Boyd, P. D. W. *J. Am. Chem. Soc.* **2000**, *122*, 10704−10705. (f) Sun, D. Y.; Tham, F. S.; Reed, C. A.; Chaker, L.; Boyd, P. D. W. *J. Am. Chem. Soc.* **2002**, *124*, 6604−6612. (g) Vinodh, M.; Alipour, F. H.; Mohamod, A. A.; Al-Azemi, T. F. *Molecules* **2012**, *17*, 11763−11799. (h) Grimm, B.; Schornbaum, J.; Cardona, C. M.; van Paauwe, J. D.; Boyd, P. D. W.; Guldi, D. M. *Chem. Sci.* **2011**, *2*, 1530−1537.
(12) (a) Boyd, P. D. W.; Hodgson, M. C.; Rickard, C. E. F.; Oliver, A. G.; Chaker, L.; Brothers, P. J.; Bolskar, R. D.; Tham, F. S.; Reed, C. A. *J. Am. Chem. Soc.* **1999**, *121*, 10487−10495. (b) Dietel, E.; Hirsch, A.; Eichhorn, E.; Rieker, A.; Hackbarth, S.; Röder, B. *Chem. Commun.* **1998**, 1981−1982. (c) Wu, Z.-Q.; Shao, X.-B.; Li, C.; Hou, J.-L.; Wang, H.; Jiang, X.-K.; Li, Z.-T. *J. Am. Chem. Soc.* **2005**, *127*, 17460−17468. (d) Solladié, N.; Walther, M. E.; Gross, M.; Figueira Duarte, T. M.; Bourgogne, C.; Nierengarten, J. F. *Chem. Commun.* **2003**, 2412−2413.
(13) Blondeau, P.; Segura, M.; Pérez-Fernández, R.; de Mendoza, J. *Chem. Soc. Rev.* **2007**, *36*, 198−210.
(14) Slagt, V. F.; van Leeuwen, P. W. N. M.; Reek, J. N. H. *Chem. Commun.* **2003**, 2474−2475.
(15) Sánchez-Quesada, J. Ph.D. Thesis, Universidad Autónoma de Madrid, 1996.
(16) Blondeau, P. Ph.D. Thesis, Universidad Autónoma de Madrid, 2007.
(17) (a) Hunter, C. A.; Anderson, H. L. *Angew. Chem., Int. Ed.* **2009**, *48*, 7488−7499. (b) Ercolani, G.; Schiaffino, L. *Angew. Chem., Int. Ed.* **2011**, *50*, 1762−1768.
(18) Bhattacharya, S.; Ujihashi, N.; Aonuma, S.; Kimura, T.; Komatsu, N. *Spectrochim. Acta Mol. Biomol. Spectros.* **2007**, *68*, 495−503.
(19) (a) Rodriguez, J.; Kirmaier, C.; Holten, D. *J. Am. Chem. Soc.* **1989**, *111*, 6500−6506. (b) Moravec, D. B.; Lovaasen, B. M.; Hopkins, M. D. *J. Photochem. Photobiol., A* **2013**, *254*, 20−24.
(20) (a) Fuhrhop, J.-H.; Mauzerall, D. *J. Am. Chem. Soc.* **1969**, *91*, 4174. (b) Ehli, C. Ph.D. Thesis, Friedrich-Alexander-Universität Erlangen-Nürnberg, 2009. (c) Gasyna, Z.; Browett, W. R.; Stillman, M. J. *Inorg. Chem.* **1985**, *24*, 2440−2447. (d) Wasieleswski, M. R.; Gaines, G. L., III; O'Neil, M. P.; Svec, W. A.; Niemczyk, M. P.; Prodi, L.; Gosztola, D. In *Dynamics and Mechanisms of Photoinduced Electron Transfer and Related Phenomena*; Mataga, N.; Okada, T.; Masuhara, H., Eds.; Elsevier Science Publishers: New York, 1992.
(21) Lawson, D. R.; Feldheim, D. L.; Foss, C. A.; Dorhout, P. K.; Elliott, C. M.; Martin, C. R.; Parkinson, B. *J. Electrochem. Soc.* **1992**, *139*, L68−L71.
(22) (a) Schuster, D. I.; Cheng, P.; Jarowski, P. D.; Guldi, D. M.; Luo, C.; Echegoyen, L.; Pyo, S.; Holzwarth, A. R.; Braslavsky, S. E.; Williams, R. M.; Klihm, G. *J. Am. Chem. Soc.* **2004**, *126*, 7257−7270. (b) Marcus, R. A. *J. Chem. Phys.* **1956**, *24*, 966−978. (c) Marcus, R. A.; Sutin, N. *Biochim. Biophys. Acta* **1985**, *811*, 265−322. (d) Marcus, R. A. *Angew. Chem.* **1993**, *105*, 1161−1172.